

See discussions, stats, and author profiles for this publication at: <https://www.researchgate.net/publication/252106803>

# Capillary force induced assembly of high aspect-ratio polymeric micropillar arrays

ARTICLE · MARCH 2010

---

READS

38

# Capillary-Force-Induced Clustering of Micropillar Arrays: Is It Caused by Isolated Capillary Bridges or by the Lateral Capillary Meniscus Interaction Force?

Dinesh Chandra and Shu Yang\*

Department of Materials Science and Engineering, University of Pennsylvania, 3231 Walnut Street, Philadelphia, Pennsylvania 19104

Received May 14, 2009. Revised Manuscript Received July 22, 2009

Because of their increased mechanical compliance, arrays of high-aspect-ratio microstructures are susceptible to deformation by capillary forces. In the literature, the collapse of a 1D array of tall line patterns during liquid evaporation off of their surface has been attributed to the Laplace pressure difference due to isolated capillary bridges. The same argument has often been simply extended to 2D arrays of tall microstructures to explain the collapse behavior. Using a short-chain polystyrene (PS) melt as a wetting liquid on a 2D array of epoxy micropillars, we showed that the collapse occurred while the micropillars were still completely surrounded by liquid, thus the clustering of micropillars should be caused by the lateral capillary meniscus interaction force rather than by often-reported isolated capillary bridges. We showed that the capillary meniscus interaction force was more than an order of magnitude smaller than that calculated from the Laplace pressure difference due to isolated capillary bridges. This result suggested a much lower critical elastic modulus for stable micropillar arrays, which agreed well with our experimental observation.

The continuous drive toward the miniaturization of electronic, mechanical, fluidic, and sensor devices presents great challenges in maintaining the stability of the fabricated nano- and microstructures in both fabrication and postfabrication stages. With decreasing sizes, the surface area to volume ratio of the features increases, resulting in the dominant effect of surface forces such as adhesion, friction, and capillary forces, which in turn impacts the long-term stability of devices. This problem becomes particularly critical in the case of dense arrays of high-aspect-ratio nano- and microstructures. Whereas the large surface area and increased mechanical compliance have been considered advantageous to high-aspect-ratio micropillar arrays for a wide range of applications, including sensors,<sup>1</sup> mechanical actuators,<sup>2</sup> biomimetic dry adhesives,<sup>3,4</sup> and tunable wetting,<sup>5</sup> these properties also lead to micropillars' increased susceptibility to deformation due to adhesion between pillars<sup>6,7</sup> and capillary forces exerted on pillars when liquid evaporates off of their surfaces.<sup>8–10</sup> Recently, the capillary force has been harnessed to self-assemble hierarchical microstructures.<sup>8,11,12</sup>

The phenomenon of the capillary force has been responsible for a wide range of macroscopic and microscopic observations ranging from the rise of liquid in a capillary tube and the clumping together of hair after a shower to the self-assembly of microparticles.<sup>13</sup> In general, the capillary force is proportional to the liquid–vapor interfacial energy  $\gamma$  and results from the tendency of a system to minimize the sum of the three interfacial energies (liquid–vapor ( $\gamma$ ), solid–vapor ( $\gamma_{sv}$ ), and solid–liquid ( $\gamma_{sl}$ )), which are related to each other through Young's equation

$$\gamma_{sv} - \gamma_{sl} - \gamma \cos \theta = 0 \quad (1)$$

where  $\theta$  is the equilibrium contact angle. However, the exact expression for the capillary force depends on the actual geometry of the system, giving rise to a range of phenomena such as the distortion of photoresist patterns due to the negative Laplace pressure of the capillary bridge,<sup>14,15</sup> the buckling of microfilaments due to liquid surface tension along the three-phase contact line,<sup>16</sup> the coalescence of fibers driven by the reduction in the liquid–vapor surface area,<sup>17,18</sup> and the aggregation of particles partially immersed in or floating on a liquid surface as a result of lateral forces arising from capillary menisci interactions.<sup>13</sup>

When a liquid is evaporated off of the surfaces of tall microstructures, for example, a 1D array of line patterns, the distortion of such patterns has been attributed to the Laplace pressure difference due to isolated capillary bridges formed between

\*Corresponding author. E-mail: shuyang@seas.upenn.edu.

(1) du Roure, O.; Saez, A.; Buguin, A.; Austin, R. H.; Chavrier, P.; Siberzan, P.; Ladoux, B. *Proc. Natl. Acad. Sci. U.S.A.* **2005**, *102*, 2390.

(2) Evans, B. A.; Shields, A. R.; Carroll, R. L.; Washburn, S.; Falvo, M. R.; Superfine, R. *Nano Lett.* **2007**, *7*, 1428.

(3) Geim, A. K.; Dubonos, S. V.; Grigorieva, I. V.; Novoselov, K. S.; Zhukov, A. A.; Shapoval, S. Y. *Nat. Mater.* **2003**, *2*, 461.

(4) Sethi, S.; Ge, L.; Ci, L.; Ajayan, P. M.; Dhinojwala, A. *Nano Lett.* **2008**, *8*, 822.

(5) Krupenkin, T. N.; Taylor, J. A.; Schneider, T. M.; Yang, S. *Langmuir* **2004**, *20*, 3824.

(6) Hui, C. Y.; Jagota, A.; Lin, Y. Y.; Kramer, E. J. *Langmuir* **2002**, *18*, 1394.

(7) Zhang, Y.; Lo, C. W.; Taylor, J. A.; Yang, S. *Langmuir* **2006**, *22*, 8595.

(8) Chandra, D.; Taylor, J. A.; Yang, S. *Soft Matter* **2008**, *4*, 979.

(9) del Campo, A.; Greiner, C. J. *Micromech. Microeng.* **2007**, *17*, R81.

(10) Kotera, M.; Ochiai, N. *Microelectron. Eng.* **2005**, *78–79*, 515.

(11) Pokroy, B.; Kang, S. H.; Mahadevan, L.; Aizenberg, J. *Science* **2009**, *323*, 237.

(12) Segawa, H.; Yamaguchi, S.; Yamazaki, Y.; Yano, T.; Shibata, S.; Misawa, H. *Appl. Phys. A: Mater. Sci. Process.* **2006**, *83*, 447.

(13) Denkov, N. D.; Velez, O. D.; Kralchevsky, P. A.; Ivanov, I. B.; Yoshimura, H.; Nagayama, K. *Langmuir* **1992**, *8*, 3183.

(14) Stoykovich, M. P.; Cao, H. B.; Yoshimoto, K.; Ocola, L. E.; Nealey, P. F. *Adv. Mater.* **2003**, *15*, 1180.

(15) Tanaka, T.; Morigami, M.; Atoda, N. *Jpn. J. Appl. Phys.* **1993**, *32*, 6059.

(16) Cohen, A. E.; Mahadevan, L. *Proc. Natl. Acad. Sci. U.S.A.* **2003**, *100*, 12141.

(17) Bico, J.; Roman, B.; Moulin, L.; Boudaoud, A. *Nature* **2004**, *432*, 690.

(18) Py, C.; Bastien, R.; Bico, J.; Roman, B.; Boudaoud, A. *Europhys. Lett.* **2007**, *77*, 44005.

structures.<sup>14,15</sup> The same argument is often taken for granted to explain the instability of 2D arrays of high-aspect-ratio structures as well.<sup>8,9,12,19,20</sup> However, different from 1D line patterns, the 2D microstructure array should be surrounded by a continuous body of liquid. It is questionable as to whether the isolated capillary bridge analysis can be applied to 2D systems. Occasionally, it has been suggested that the collapsing behavior of 2D micropillar arrays is caused by lateral forces arising from the interaction between capillary menisci formed around the microstructures.<sup>21</sup> Nevertheless, many times there is no distinction between these two approaches in the literature.<sup>22</sup> Furthermore, the justification for employing either of the two approaches has not been provided.

In this letter, we present experimental evidence and simple theoretical analysis to show that in the case of 2D arrays of micropillars, when a liquid is evaporated off of the surface, the clustering of the micropillars should be attributed to the lateral forces resulting from capillary menisci interaction rather than the Laplace pressure difference due to isolated capillary bridges. The capillary meniscus interaction force can be more than an order of magnitude smaller than that obtained by assuming the Laplace pressure difference due to isolated capillary bridges. Consequently, the critical elastic modulus necessary for the stability of the micropillars is much smaller than that estimated by the capillary bridge approach.

To study the capillary-induced collapse behavior and visualize the liquid morphology between the micropillars, we exposed square-lattice-arrayed epoxy micropillars to a short-chain, monodisperse polystyrene (PS) melt ( $M_n = 1.79$  kg/mol and PDI = 1.06,  $T_g = 65$  °C, from PSS-Polymer Standards Service – USA Inc.), which acted as the wetting liquid on pillars. The epoxy micropillar arrays (diameter  $0.6 \mu\text{m}$ , height  $4.8 \mu\text{m}$ , and pitch  $1.5 \mu\text{m}$ ) were prepared by replica molding<sup>7</sup> from a mixture of commercially available epoxy resin (DER 354, Dow Chemical) and 3 wt % cationic photoinitiator (Cycracure UVI 6976, Dow Chemical), followed by UV curing ( $\sim 8.5$  mW/cm<sup>2</sup>) for  $\sim 30$  min. The micropillar array (Figure 1a) was then placed on a hot plate at  $180$  °C and sprinkled with a few particles of PS on the top. The PS powder quickly melted on the micropillar array, and the temperature was held at  $180$  °C for 1 h, followed by quenching to room temperature for subsequent imaging by scanning electron microscopy (SEM). Previous studies have shown that the morphology of PS remains identical before and after freezing.<sup>23,24</sup> As seen in the SEM image in Figure 1b, the micropillars collapsed while they were still completely surrounded by PS liquid. The absence of isolated capillary bridges between the micropillars and the fact that a continuous liquid body in mechanical equilibrium has a constant Laplace pressure everywhere<sup>25</sup> indicate that the Laplace pressure difference cannot be simply used here to explain the observed collapse of micropillars. It should be noted, however, that for a 1D array of line patterns the Laplace pressure argument is applicable because in that geometry isolated liquid between the lines could exist, resulting in different Laplace pressures. Atomic force microscopy (AFM) imaging of polystyrene frozen in a mechanically stable, low-aspect-ratio ( $10 \mu\text{m}$  diameter,  $10 \mu\text{m}$  height, and  $20 \mu\text{m}$  pitch) micropillar array

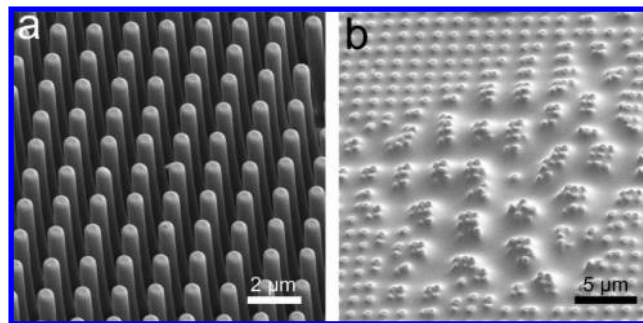


**Figure 1.** SEM images of epoxy micropillar arrays. (a) As fabricated and (b) collapsed by a polystyrene melt.

(Figure 2) further confirms that the mean curvature, and thus the Laplace pressure in the liquid surrounding the micropillars, is constant everywhere. For example, in Figure 2, the mean curvature at point A between adjacent pillars,  $(R_1^{-1} - R_3^{-1})/2$ , is equal to  $-R_2^{-1}$ , the mean curvature at point B between diagonally opposite pillars. However, even in the absence of a Laplace pressure variation, it has been suggested that when two particles are partially immersed in a liquid or float on a liquid interface they experience a lateral capillary meniscus interaction force,<sup>26</sup> which can be either attractive (when the particles are both hydrophobic or both hydrophilic) or repulsive (when the particles have opposite wettabilities). This lateral force arises because of the deformation of the otherwise flat liquid surface due to the presence of the particles. On the basis of the equations given by Kralchevsky et al.,<sup>27</sup> the expression (detailed derivation in Supporting Information) for the capillary interaction energy,  $W_c$ , of two cylinders (Figure 3a) when partially immersed in a liquid of surface tension  $\gamma$  with a contact angle  $\theta$  is given as

$$W_c = -2\pi\gamma R^2 \cos^2 \theta \ln \left( \frac{l_c}{x + \sqrt{x^2 - 4R^2}} \right) \quad (2)$$

where  $l_c = (\gamma/\rho g)^{1/2}$  is the capillary length of the liquid ( $\rho$  is the density and  $g$  is the gravitational acceleration) and  $R$  and  $x$  are as defined in Figure 3a.

The capillary force between them is

$$F_c = -\frac{dW_c}{dx} = -\frac{\pi\gamma R^2 \cos^2 \theta}{\sqrt{(x/2)^2 - R^2}} \quad (3)$$

In the case of micropillars, where one end is fixed on the substrate, the torque  $\tau_c$  on the micropillars due to  $F_c$  is

$$\tau_c = \frac{\pi\gamma R^2 h \cos^2 \theta}{\sqrt{(x/2)^2 - R^2}} \quad (4)$$

For the same geometry, in the case of an isolated capillary bridge between micropillars (Figure 3b), the Laplace pressure difference is approximately  $P_1 \approx \gamma \cos \theta / (x/2) - R$  and thus the torque on the micropillars is

$$\tau_1 \approx \frac{2R\gamma \cos \theta}{\frac{x}{2} - R} \int (h) dh = \frac{\gamma R h^2 \cos \theta}{\frac{x}{2} - R} \quad (5)$$

(19) Chakrapani, N.; Wei, B.; Carrillo, A.; Ajayan, P. M.; Kane, R. S. *Proc. Natl. Acad. Sci. U.S.A.* **2004**, *101*, 4009.

(20) Lee, T. W.; Mitrofanov, O.; Hsu, J. W. R. *Adv. Funct. Mater.* **2005**, *15*(10), 1683.

(21) Zhao, Y. P.; Fan, J. G. *Appl. Phys. Lett.* **2006**, *88*, 103123.

(22) Fan, J. G.; Dyer, D.; Zhang, G.; Zhao, Y. P. *Nano Lett.* **2004**, *4*, 2133.

(23) Seemann, R.; Herminghaus, S.; Jacobs, K. *Phys. Rev. Lett.* **2001**, *87*, 196101.

(24) Seemann, R.; Brinkmann, M.; Kramer, E. J.; Lange, F. F.; Lipowsky, R. *Proc. Natl. Acad. Sci. U.S.A.* **2005**, *102*, 1848.

(25) de Gennes, P. G.; Brochard-Wyart, F.; Quere, D. *Capillarity and Wetting Phenomena*; Springer: New York, 2004.

(26) Kralchevsky, P. A.; Nagayama, K. *Particles at Fluid Interfaces and Membranes*; Elsevier: Amsterdam, 2001.

(27) Kralchevsky, P. A.; Paunov, V. N.; Ivanov, I. B.; Nagayama, K. *J. Colloid Interface Sci.* **1992**, *151*, 79.

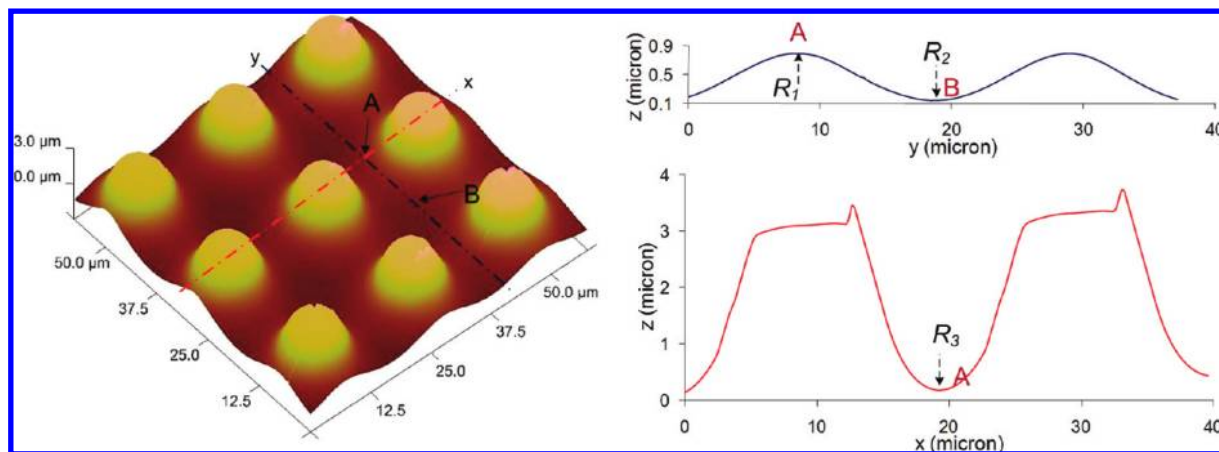


**Figure 2.** AFM scan of polystyrene wetting morphology in epoxy micropillar arrays. The mean curvature at two representative points, A and B, is the same.

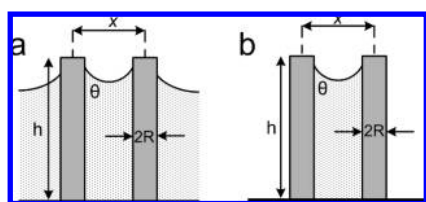


**Figure 3.** Schematic illustrations of two micropillars (a) partially immersed in a liquid and (b) with an isolated capillary bridge between them.

The ratio of the torques calculated by two approaches is

$$\frac{\tau_1}{\tau_c} \approx \frac{h}{\pi R \cos \theta} \sqrt{\frac{\frac{x}{2} + R}{\frac{x}{2} - R}} \quad (6)$$

Thus, according to eq 6, for a typical case of  $\theta = 60^\circ$  and an aspect ratio of 10, the torque in the case of isolated capillary bridge is at least 12 times greater than that from lateral capillary meniscus interaction.

The large difference in the torques calculated from the two approaches is reflected in a large difference in the critical elastic modulus for the stability of micropillar arrays when estimated from the two approaches. The critical modulus calculated from the capillary meniscus interaction approach is significantly smaller than that calculated from the isolated capillary bridge approach. It has been observed by us and others that in the case of micropillars arranged in a square lattice the collapse due to the evaporation of liquid is initiated by groups of four neighboring pillars clustering together.<sup>11,21,28</sup> Thus, in a simple model we consider four pillars on the corners of a square as shown in the Figure 4a inset. Let the pillars come together by deflection  $\delta$  in both directions. In this configuration, assuming the superposition of pairwise interaction between the micropillars, the capillary meniscus interaction force  $F_C$  acting on a micropillar is given by

$$F_C = \frac{\pi \gamma d^2 \cos^2 \theta}{2} \left( \sqrt{\frac{2}{(p-2\delta)^2 - d^2}} + \sqrt{\frac{1}{2(p-2\delta)^2 - d^2}} \right) \quad (7)$$

The elastic restoring force acting on the deflected pillar is given as<sup>29</sup>

$$F_E = \frac{3\sqrt{2}\pi E d^4 \delta}{64h^3} \quad (8)$$

The critical modulus for stability,  $E_{\text{crit}}$ , can be obtained when  $F_E \geq F_C$ . A typical plot of  $F_C$  and  $F_E$  (Figure 4a) shows that this condition is satisfied for some critical deflection  $\delta_c$  when the curve for  $F_E$  is at least tangential to the curve for  $F_C$ . Thus, the value of  $\delta_c$  is obtained by solving  $dF_C/d\delta = F_C/\delta$  in terms of  $\delta$ . Putting the value of  $\delta_c$  back into eqs 7 and 8 and then solving  $F_E = F_C$  in terms of  $E$  gives  $E_{\text{crit}}$  as

$$E_{\text{crit}} = \frac{32\sqrt{2}\gamma \cos^2 \theta h^3}{3d^4} f(r) \quad (9)$$

where  $f(r)$  is a function of  $r = p/d$  and is plotted in Figure 4b:

$$f(r) = \frac{1}{r-k} \left( \sqrt{\frac{2}{k^2-1}} + \sqrt{\frac{1}{2k^2-1}} \right) \quad (10a)$$

$$r = \frac{1}{k} \left( \frac{\sqrt{2}(k^2-1)^{-1/2} + (2k^2-1)^{-1/2}}{\sqrt{2}(k^2-1)^{-3/2} + 2(2k^2-1)^{-3/2}} \right) + k \quad (10b)$$

It should be noted that  $E_{\text{crit}}$  is the minimum modulus below which micropillars will always be unstable ( $F_C > F_E$ ) for all deflection values  $\delta$ . For stable pillars, the elastic modulus  $E$  should be considerably greater than  $E_{\text{crit}}$  such that  $F_E > F_C$  is maintained over a reasonable range of deflection,  $\delta_1$  (stable equilibrium) to  $\delta_2$  (unstable equilibrium) (Figure 4a). Because the capillary force between the micropillars (eqs 3 and 7) diverges as the micropillar separation tends to zero, the model predicts that regardless of the value of elastic modulus  $E$ , for deflection values greater than  $\delta_2$ ,  $F_C > F_E$ . In practice, though, in the absence of other external forces, which may cause the micropillars to deflect beyond  $\delta_2$  to start with, stability can be ensured if  $F_E > F_C$  is maintained over a reasonable range of deflection,  $\delta_1$  to  $\delta_2$ .

To validate the expression derived for  $E_{\text{crit}}$  in eq 9, we fabricated square-lattice micropillar arrays (diameter 0.75  $\mu\text{m}$ , height 9  $\mu\text{m}$ , and pitch 1.5  $\mu\text{m}$ ) with different elastic moduli and investigated their capillary-force-induced collapse.

(28) Chandra, D.; Yang, S.; Soshinsky, A.; Gambogi, R. *ACS Appl. Mater. Interf.* **2009**, doi: 10.102/am900253z.

(29) Beer, F. B.; Johnston, E. R. *Mechanics of Materials*, 2nd ed.; McGraw-Hill: New York, 1992.



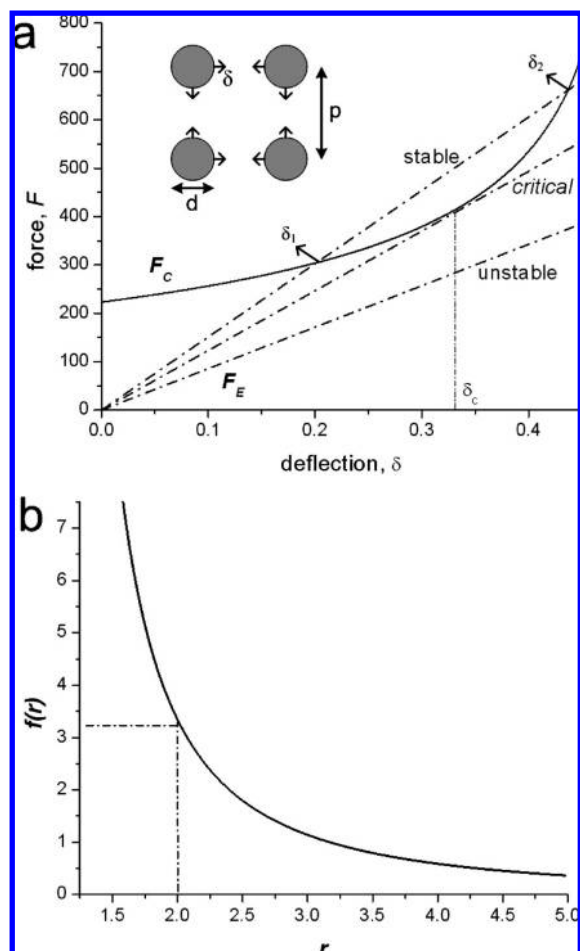


**Figure 4.** (a) Typical plot of the capillary interaction force,  $F_C$  (solid line), and elastic restoring force acting on the deflected pillar,  $F_E$  (dashed lines).  $\delta_1$  and  $\delta_2$  represent stable equilibrium and unstable equilibrium, respectively. (Inset) Schematic illustration of the interaction among a group of four pillars. The increasing slope of  $F_E$  corresponds to increasing elastic modulus  $E$ . (b) Function  $f(r)$  is a function of  $r = p/d$ . The dashed line indicates the value of the function at  $r = 2$ .

Micropillar arrays were fabricated by molding copolymers from 2-hydroxyethyl methacrylate (HEMA) and methyl methacrylate (MMA) using a procedure described in our earlier publication.<sup>8,28</sup> The micropillars were collapsed by evaporating water off of their surface. We modulated the elastic modulus of the micropillars in the wet state by varying the relative composition of water-swallowable poly(2-hydroxyethyl methacrylate) (PHEMA) and glassy poly(methyl methacrylate) (PMMA). The elastic moduli in the wet state were determined by atomic force microscope (AFM) nanoindentation in a fluid cell.<sup>28,30</sup> The SEM images (Figure 5) of the micropillar arrays after water evaporation off of their surface show that the micropillars are unstable when the elastic modulus is 745 MPa (67 wt % PMMA) or less but stable when the elastic modulus is 1.2 GPa (75 wt % PMMA). From eq 9,  $E_{\text{crit}}$  is calculated to be 714 MPa, which is consistent with experimental observation. Here, the water contact angle  $\theta$  was measured to be  $73^\circ$ . In comparison, for the same geometry, the critical elastic modulus,  $E'_{\text{crit}}$ , according to the Laplace pressure difference due to the isolated capillary bridge between the four

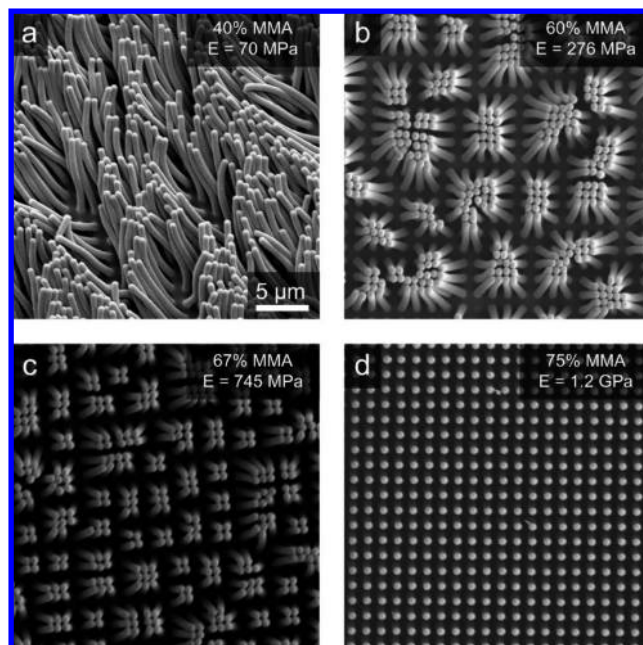


**Figure 5.** SEM images of the collapse behavior of PHEMA-co-PMMA micropillars with different elastic moduli by the water capillary force upon evaporation of water. The scale bar in image a applies to all images.

pillars is given by<sup>8,15</sup>

$$E'_{\text{crit}} = \frac{128\gamma h^3 (3h \cos \theta + w \sin \theta + \sqrt{9h^2 \cos^2 \theta + 3hw \sin(2\theta)})}{3\pi d^3 w^2} \quad (11)$$

Here,  $w = p\sqrt{2} - d$  is the spacing between the diagonally opposite micropillars. From eq 11,  $E'_{\text{crit}}$  is calculated to be 16.7 GPa, which is much greater than the 1.2 GPa value for which the micropillars were found to be stable experimentally. Furthermore, by using the capillary meniscus interaction force approach established here, we have successfully predicted the micropillar cluster size as a function of elastic modulus.<sup>28</sup>

The above analysis for the critical elastic modulus convincingly confirms that in 2D arrays of tall microstructures the capillary meniscus interaction, rather than the Laplace pressure difference due to isolated capillary bridges, is the main reason for mechanical instability upon liquid drying. It must be pointed out, though, that in later stages of liquid evaporation there may no longer be a continuous liquid body surrounding the micropillars and isolated capillary bridges may likely form. However, such isolated capillary bridges will be near the base of the micropillars and thus will exert much less torque than a capillary bridge spanning the whole micropillar length.

In conclusion, we have investigated the capillary force responsible for the collapse of 2D arrays of tall microstructures upon liquid evaporation. Our theoretical analysis and comparison to experimental results suggest that the capillary meniscus interaction force is mainly responsible for the pillar collapse rather than the often-cited Laplace pressure difference due to isolated capillary bridges. For a given geometry, the capillary meniscus interaction force exerted on micropillar arrays is much smaller than the force due to isolated capillary bridges; therefore, a much smaller critical elastic modulus is required for the stability of the microstructures. The quantitative analysis presented here will

(30) Domke, J.; Radmacher, M. *Langmuir* **1998**, *14*, 3320.

be important for the rational design of stable arrays of tall microstructures or harnessing such instability for various applications.<sup>11,28</sup>

**Acknowledgment.** This work is in part supported by the National Science Foundation (CAREER/DMR-0548070 and MRSEC/DMR-0520020). We acknowledge the Penn Regional Nanotechnology Facility for access to AFM nanoindentation and

SEM. We thank Krishnacharya Khare for helpful discussion about the use of low-molecular-weight polystyrene.

**Supporting Information Available:** Derivation of the capillary meniscus interaction energy of two cylinders partially immersed in a liquid (eq 2) from the equations in ref 27. This material is available free of charge via the Internet at <http://pubs.acs.org>.